(30) Equation IV-5 is applicable also to cylindrical microdomains.[31]
(31) Mori, K.; Hasegawa, H.; Hashimoto, T.; Kawai, H., to be submitted to *Macromolecules*.
(32) Scott, R. L. *J. Chem. Phys.* **1949**, *17*, 279.
(33) Todo, A.; Hashimoto, T.; Kawai, H. *J. Appl. Crystallogr.* **1978**, *11*, 558.
(34) It was pointed out by a reviewer that the presence of methylene chloride could lower the vapor pressure of the DOP and allow substantial evaporation of the DOP as the methylene chloride is removed. Although the DOP concentration levels in the systems were not studied by an independent means in this work, one may have to bear in mind this effect for more quantitative studies.
(35) It should be noted in Figure 4 that the widths of the first-order and second-order peaks remain essentially constant with increasing temperature, despite the fact that the higher order peaks (the third- and fourth-order peaks) disappear with increasing temperature. This fact strongly suggests that the disappearance of the higher order peaks with increasing temperature is due to the increasing interfacial thickness but not to the disordering of the lattice structure or the smallness of the grain structure within which the orientation of lamellae is coherent, as is the case in the wide-angle X-ray diffraction. The effect of the interfactial thickness on the SAXS profile is given by

$$I(s;\sigma) = I(s;\sigma=0) \exp(-4\pi^2\sigma^2 s^2)$$

where σ is the parameter characterizing the thickness of the diffuse interphase and $I(s;\sigma=0)$ is the scattered intensity for the system having zero interfacial thickness. Thus the greater the scattering angle, the larger the intensity decay due to the finite interfacial thickness σ.[7,24,36]
(36) Hashimoto, T.; Kowsaka, K.; Shibayama, M.; Kawai, H., to be submitted to *Macromolecules*; *Polym. Prepr., Am. Chem. Soc., Div. Polym. Chem.* **1983**, *24* (2).
(37) It should be noted that an effect of thermal expansion should increase the domain size and domain identity period D with increasing temperature. However, this effect is trivial and much outweighed by the effect of segregation power. The effect of the different thermal expansion coefficients in both phases in the phase-separated systems may vary the scattering contrast, affecting the scattered intensity. However, this effect is again much outweighed by the effect of the segregation power.
(38) The "grain" refers to a region in wich the orientation of the lamellar microdomains is coherent. Increasing segregation power accompanied by increasing concentration involves deformation of the grain in such a way that its dimension normal to the interface should expand but the dimensions parallel to it shrink.

Microphase Structure of Solvent-Cast Diblock Copolymers and Copolymer–Homopolymer Blends Containing Spherical Microdomains

Frank S. Bates,† C. V. Berney, and R. E. Cohen*

Department of Chemical Engineering, Massachusetts Institute of Technology, Cambridge, Massachusetts 02139. *Received October 27, 1982*

ABSTRACT: Investigated in this work were the effects of solvent-casting conditions, the presence of homopolymer in the continuous phase, and the magnitude of block molecular weights on the structural features of styrene–butadiene diblock copolymers and diblock copolymer–homopolystyrene blends containing spherical domains of polybutadiene. Domain boundary thickness, domain size, and domain packing order were determined from small-angle neutron scattering (SANS) measurements. Domain boundary thickness was essentially identical for all samples and in agreement with theory. Contrary to theory, sphere radius was found to be proportional to the 0.37 power of polybutadiene molecular weight; this is shown to be an artifact of the solvent-casting process. Under equilibrium conditions, the domains form a body-centered-cubic paracrystalline macrolattice which is disrupted by the addition of homopolystyrene.

Introduction

Block copolymer structure and properties have generated considerable scientific interest over the past 2 decades. Recent years have found significant advances made in the study of morphology, in large part due to the growing popularity of small-angle scattering techniques. Hashimoto et al.[1–6] have been particularly active in this area, examining polystyrene–vinylpolyisoprene diblock copolymers containing lamellar and spherical (rubber) microdomains by small-angle X-ray scattering (SAXS). Their results leave several unanswered questions with respect to the spherical morphology. For example, these authors found the domain radius to be almost half that predicted from theory,[7] which they contend is a result of the process of solvent casting. Also, no specific domain packing order could be clearly established for their samples.

The present paper is part of a larger study designed to examine relationships between microphase structure and mechanical behavior in block copolymers and polymer blends. Five polystyrene–polybutadiene diblock copolymers and seven diblock copolymer–homopolystyrene blends have been prepared, three of these containing perdeuterated polybutadiene and all exhibiting a morphology consisting of polybutadiene microspherical domains.

The structural features of these materials have been investigated by small-angle neutron scattering (SANS), exploiting the enhanced contrast that results from the use of deuterated butadiene. We presently report on the domain order, domain size (also determined by electron microscopy), and domain boundary thickness in solvent-cast films; homopolystyrene content and block molecular weights are the major variables of the study. SANS determination of the polybutadiene block single-chain behavior has been reported separately.[8] The dynamic mechanical properties of these materials and their relationship to the presently detailed structures are reported in the accompanying paper immediately following this one.

Experimental Section

Materials. Styrene monomer (Aldrich Chemical Co.) was deinhibited by washing with 10% NaOH followed by distilled water and was stored over CaH_2 at 0 °C. Prior to use, the styrene was distilled and redistilled from fresh Na wire and used within 2 h.

1,3-Butadiene (Matheson, high purity) was deinhibited with a 10% NaOH solution, dried over NaOH pellets and molecular

† Present address: Bell Laboratories, Murray Hill, NJ 07974.

0024-9297/83/2216-1101$01.50/0

Table I
Molecular Characterization Results

sample[a]	$10^{-3}M_{n,S}$[b]	$10^{-3}M_{n,B}$[c]	$(M_w/M_n)_{SB}$
SB1	79	11	1.06
SB2	77	21	1.06
SB3	85	45	1.07
SB4	149	20	1.07
SB5	126	46	1.06
SB6	122	66	1.07
SB7	560	59	1.11
SB8	450	123	1.15
SB9	420	230	1.12
SB_d1	80	13	1.07
SB_d2	78	54	1.10
SB_d3	380	46	1.10
S1	64		1.06
S2	116		1.05
S3	390		1.05
B1		20	1.04

[a] The subscript d signifies a perdeuterated polybutadiene block. [b] Number-averaged molecular weight of the styrene block determined by HPSEC. [c] Number-averaged molecular weight of the butadiene block determined by HPSEC and UV absorption.

sieves, and condensed and stirred over CaH_2 at 0 °C for 24 h. The butadiene was then condensed over several Na mirrors and was frozen until use.

1,3-Butadiene-d_6 (Merck Sharp and Dohme, Ltd.) was stirred over CaH_2 at 0 °C for 24 h, condensed over several Na mirrors, and frozen until use. The reported 98 atom % deuterium was verified by mass spectrometry.

n-Butyllithium (Aldrich) was used as received or diluted with cyclohexane and in each case was titrated by a modified[9] Eppley and Dixon[10] method. Reagent grade benzene (J. T. Baker Co.) was distilled twice under argon, followed by the addition of a small amount of anisole (5–10 times the concentration of initiator used in the later polymerization).[11] The mixture was then further purified by a previously reported "living gel" technique.[12]

The solvents used for film casting were reagent grade toluene, benzene, tetrahydrofuran (THF), and methyl ethyl ketone (MEK); each was used as received from J. T. Baker Co.

Polymer Synthesis and Characterization.[9] Diblock copolymerizations were carried out under highly purified argon in a Pyrex reactor fitted with grease-free connectors and valves. Benzene, initiator, and styrene were added to the reactor and vigorously stirred for several hours at 40 °C. Following removal of a small sample for later analysis, the butadiene was introduced to the reactor and the temperature was raised to 50 °C. After several hours, the reaction was terminated with methanol. Homopolystyrene was prepared in the same manner as block polystyrene and terminated with methanol. The polymers were precipitated with methanol, dried under vacuum for several days, and stored at −20 °C. A total of twelve diblock copolymers, three of which contained fully deuterated polybutadiene blocks, plus a polybutadiene and three polystyrene homopolymers were prepared as described above.

Diblock copolymer composition was determined by ultraviolet (UV) absorption in chloroform (Mallinckrodt, Inc.) at a wavelength of 262 nm; in each case the UV result was in good agreement with the synthesis stoichiometry. Block polystyrene (sampled from the reactor), homopolystyrene, and diblock copolymer samples were analyzed by high-pressure size exclusion chromatography (HPSEC) employing a set of Zorbax PSM bimodal columns with toluene as the mobile phase. The HPSEC instrument was calibrated with nine polystyrene standards (Polysciences, Inc.); this provides for the direct determination of polystyrene sample molecular weight, $M_{n,S}$. In each case the polystyrene heterogeneity index (M_w/M_n), as measured by HPSEC, was between 1.05 and 1.08. Block polybutadiene molecular weight, $M_{n,B}$, was calculated from the HPSEC block polystyrene molecular weight and the UV absorption composition. Diblock copolymer heterogeneity, $(M_w/M_n)_{SB}$, was also determined directly by HPSEC. $M_{n,S}$, $M_{n,B}$, and $(M_w/M_n)_{SB}$ are listed in Table I.

Table II
Electron Microscopy Results

	weight fraction		domain size, Å		
sample	SB	S	R_{pred}[a]	$\bar{R}_{EM}$[b]	$\sigma_R/\bar{R}$[c]
SB1	1.00		129	117	0.07
SB2/S2	0.52	0.48	199	159	0.08
SB3/S1	0.35	0.65	333	231	0.13
SB4	1.00		193	152	0.09
SB5/S2	0.49	0.51	340	200	0.07
SB6/S2	0.34	0.66	430	243	0.07
SB7	1.00		394	243	0.09
SB8/S3	0.52	0.48	647	298	0.12
SB9/S2	0.34	0.66	1032	355	0.07
SB_d1	1.00		137	122	0.06
SB_d2/S1	0.35	0.65	357	224	0.08
SB_d3	1.00		309	177	0.07
SB_d3/S2/B1	0.50	0.44[d]		247	0.42

[a] Calculated from the formulas of Helfand and Wasserman,[7] assuming blends are pure diblock copolymers containing the actual polybutadiene molecular weight. [b] 1.3 times the values obtained by measuing electron micrographs (see ref 16). [c] Determined from measurements of approximately 100 domains per micrograph. [d] Weight fraction B = 0.06.

The hydrogenated polybutadiene microstructure was determined by proton NMR to be 87% mixed cis and trans 1,4 and 13% 1,2 addition. As reported elsewhere,[9] the perdeuterated polybutadiene exhibits the same glass transition temperature as the hydrogenous analogue, indirectly verifying the expected similarity in microstructure.

Sample Preparation. The diblock copolymer samples appearing in Table I fall into three categories: ~12%, ~23%, and ~36% by weight polybutadiene. Those containing ~23% and ~36% rubber were blended with homopolystyrene as reported in Table II so that all test specimens contained approximately 12% rubber. Film specimens used for SANS and EM analysis were prepared by a solvent spin-casting technique[9,13] (see also the paper immediately following this one), starting with 2–5% solutions of the polymer in either toluene, benzene, or a mixture composed of 70% tetrahydrofuran and 30% methyl ethyl ketone (THF/MEK). Solvent was removed over a period of several days while a nitrogen atmosphere was maintained within the casting chamber. When toluene was the solvent, casting was done at 80 °C. Samples were cast from benzene and THF/MEK starting at 60 and 50 °C, respectively, and the temperature was increased to 80 °C during the course of solvent removal. Uniform thin films (approximately 0.05 cm) were obtained in this manner. Films were annealed under vacuum from 24 h at 120 °C, cooled (~20 °C/h) to room temperature, and stored in the dark under vacuum. Samples subjected to SANS analysis were reannealed several days prior to their examination.

Structural Analysis. Electron micrographs were obtained on a Phillips 200 electron microscope (EM) operated at either 60 or 80 kV and calibrated against a diffraction grating carbon replica (21 600 lines/cm). Samples were stained with osmium tetraoxide[14] and sectioned on a LKB ultramicrotome fitted with a freshly prepared glass knife.

Small-angle neutron scattering (SANS) experiments were performed on the 30-m instrument at the National Center for Small-Angle Scattering Research (NCSASR), Oak Ridge National Laboratory,[15] employing neutrons of 4.75-Å wavelength and sample-to-detector distances ranging from 1.8 to 15.3 m. SANS results were obtained from four-layer samples that were approximately 0.2 cm thick. One 0.05-cm-thick specimen was also examined. Scattering data have been corrected for background scattering and detector sensitivity. Details concerning pinhole sizes, scattering geometry, sample transmission, and detector settings of individual spectra have been reported elsewhere.[9]

Results

Electron microscopy of sample SB6/S2 cast from toluene revealed a cylindrical polybutadiene microstructure,

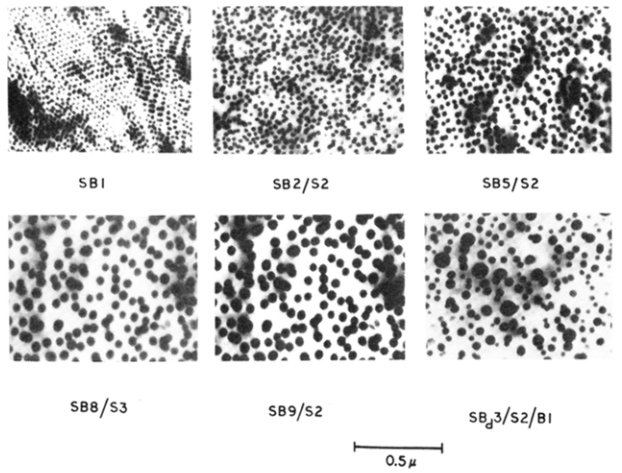

Figure 1. Electron micrographs of solvent-cast polystyrene–polybutadiene diblock copolymers and blends. Samples were stained with osmium tetraoxide, which preferentially darkens the polybutadiene domains.

while the same sample cast from THF/MEK contained spherical microdomains of polybutadiene. Therefore, all samples containing homopolystyrene were cast from THF/MEK in order to ensure a spherical morphology. Unblended diblock copolymer films (Table II) prepared from each of the three casting solvents exhibited a spherical morphology; presently reported EM results were obtained from toluene-cast samples. The effect of casting solvent on structure was determined by SANS as discussed in the following sections. Micrographs from five representative samples listed in Table II are presented in Figure 1. The morphology of a sixth sample, designated SB$_d$3/S2/B1, is also shown in Figure 1; this ternary blend of a diblock copolymer and both homopolymers is discussed in detail in the following paper on mechanical properties of these materials. Sphere radii and standard deviations were calculated[16] from representative populations of approximately 100 domains and are listed in Table II.

Table III
Neutron Scattering Lengths and Scattering-Length Densities

monomer	$10^{12}b$, cm	$10^{-10}\rho_b$, cm·cm^{-3}
styrene	2.328	1.416
butadiene	0.416	0.415
butadiene-d_6	6.66	6.65

Three characteristic SANS spectra are presented in Figure 2 in the form of intensity contour plots, along with electron micrographs taken from the corresponding samples. All samples examined were found to scatter isotropically as demonstrated by Figure 2. Therefore SANS data have been radially averaged and are reported in units of relative intensity, $I(Q)$ ($Q = 4\pi\lambda^{-1}\sin\theta$, where λ is the radiation wavelength and θ equals half the scattering angle).

SANS Analysis

We have examined three structural features present in the materials given in Table II by means of SANS: domain boundaries, domain sizes, and domain packing. These are treated separately below since they represent the dominant mechanism of scattering in separate regions of momentum transfer Q.

Domain Boundary. The domain boundary thickness of a two-phase material can be determined by using the Porod region of a small-angle scattering curve. As detailed by Koberstein et al.,[17] diffuse phase boundaries produce deviations from Porod's law, which can be represented by

$$I_{obsd}(Q) = \frac{K_p}{Q^4}H^2(Q) \qquad (1)$$

$$K_p = 2\pi A_i(\rho_{bp} - \rho_{bm})^2$$

where A_i is the total interfacial area of the system and ρ_{bp} and ρ_{bm} are the scattering-length densities (Table III) of the particles and matrix, respectively. $H(Q)$ is the Fourier transform of a smoothing function that, when convoluted

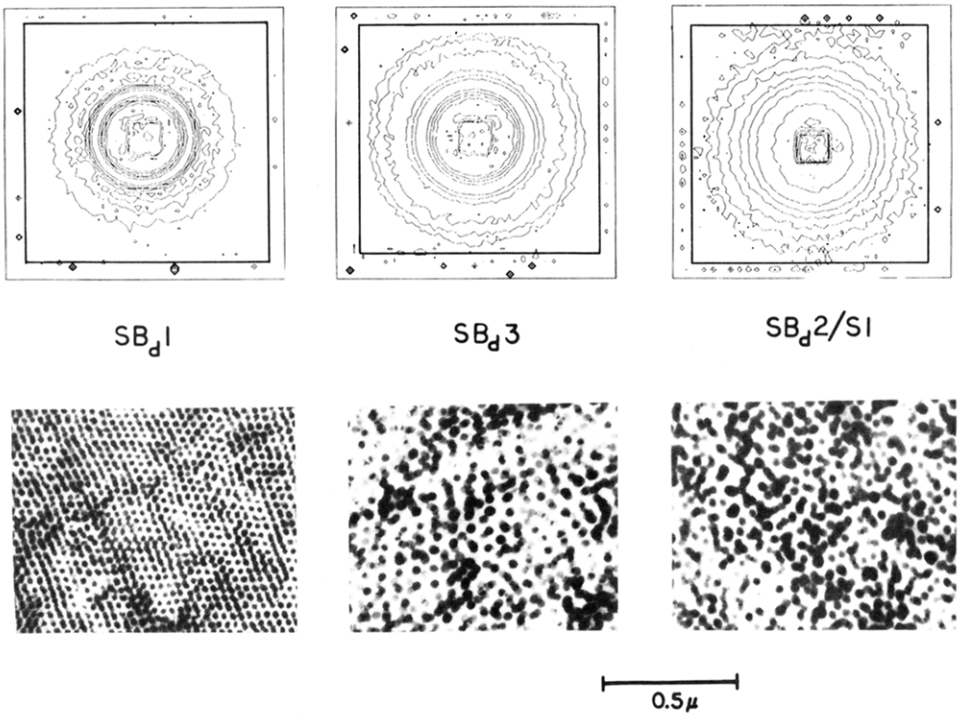

Figure 2. Contour plots of SANS intensities for typical samples, together with the corresponding electron micrographs. The circular rings confirm the isotropic nature of the samples (the square object in the center is the beamstop).

Table IV
SANS Results

sample[a]	domain boundary thickness (Å) ± 10% ΔR	a_I	domain size $\bar{R}$, Å	$\sigma_R/\bar{R}$	domain packing $\bar{D}$, Å	domains/paracrystal
SB_d1-T	20	14	124 ± 2	0.11 ± 0.01	347 ± 2	110
SB_d1-B	21	14	121 ± 2	0.13 ± 0.01	345 ± 2	172
SB_d1-M	20	14	124 ± 3	0.12 ± 0.02	340 ± 3	124
SB_d1-M[b]	21	14				
SB1-T			117[c]		325 ± 2	241
SB_d3-T	23	15	197 ± 3	0.11 ± 0.01	635 ± 4	40
SB_d3-B	23	16	196 ± 3	0.11 ± 0.01	638 ± 4	36
SB_d3-M	23	16	181 ± 3	0.09 ± 0.02	579 ± 4	42
SB7-T			222 ± 3	0.11 ± 0.01		
SB_d2/S1-M	22	15	221 ± 3	0.10 ± 0.01	690 ± 5	5

[a] Casting solvent: T = toluene, B = benzene, M = THF/MEK. [b] Sample thickness = 0.05 cm. [c] Calculated from UV composition and Bragg spacing assuming a bcc packing mode.[26]

with a step profile, produces the diffuse scattering-length density profile. Two such interfacial composition profiles are considered. The first, introduced by Ruland[18] and used extensively by Hashimoto et al.,[1-6] is obtained from a Gaussian smooth function of standard deviation σ, which results in the following version of eq 1:

$$I_{obsd}(Q) = \frac{K_p}{Q^4} \exp(-\sigma^2 Q^2) \quad (2)$$

The parameter σ, which provides a measure of interfacial thickness (see Discussion), can be determined from a plot of ln (IQ^4) vs. Q^2.

The second profile corresponds to that predicted by Helfand and Wasserman,[7,19] for which[19]

$$I_{obsd}(Q) = \frac{K_p}{Q^4}\left(\frac{\pi a_I Q/4}{\sinh(\pi a_I Q/4)}\right)^2 \quad (3)$$

where a_I is defined as the interfacial thickness (see Discussion). Equation 3 can be series expanded to give

$$I_{obsd}(Q) = \frac{K_p}{Q^4}\left(1 - \frac{(\pi a_I Q/4)^2}{3} + \mathcal{O}(Q^4)\ldots\right) \quad (4)$$

from which a_I can be determined by plotting IQ^2 vs. Q^{-2}.

In order to apply eq 2 and 4 to SANS data, one must first subtract the incoherent scattering contributing to the recorded intensity. The procedure for determining this correction is illustrated in Figure 3. For $Q > 0.15$ Å^{-1}, all scattering curves were found to be linear and nearly independent of Q; that is, one observes only incoherent scattering. Sample S3 (polystyrene homopolymer) serves to demonstrate that in the absence of any known heterogeneities, this behavior in fact persists to a low value of Q; note that the heterogeneous samples contain ~88% polystyrene. Therefore, for values of $Q < 0.15$ Å^{-1}, the incoherent scattering intensity can be estimated from an extrapolation of a linear regression of the data at higher Q. A similar procedure is routinely employed in SAXS, although in the case of X-rays, the background intensity is due to thermal diffuse scattering and the correction must be developed as a power series in Q.[20,21] Incoherent background corrections are given in Figure 3 by the solid lines. The slight slope associated with incoherent scattering is instrument related[22] and has been shown to have no effect on the domain boundary thickness calculations.[9]

Typical plots, based on eq 2 and 4, for deuterium-labeled samples are shown in Figure 4. The quantities σ and a_I have been determined from least-squares linear regressions in which each point has been weighted with its associated variance. The results are listed in Table IV, where the

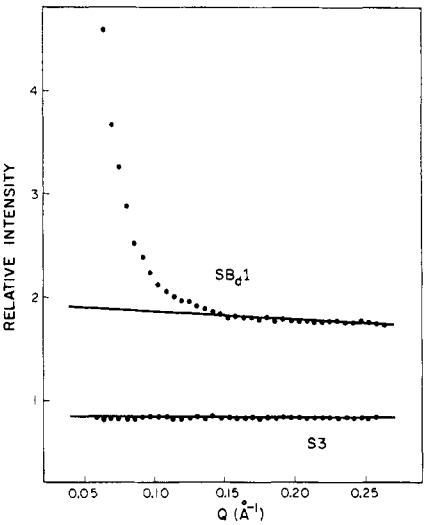

Figure 3. Radially averaged SANS intensities for samples SB_d1 and S3 (homopolystyrene). Straight lines fitted to the high-Q data are used to determine the incoherent scattering correction.

convention established by Hashimoto et al.[2] for defining the interfacial thickness (based on a Gaussian smoothing-function model) has been adopted:

$$\Delta R = (2\pi)^{1/2}\sigma \quad (5)$$

Domain Size. Intraparticle scattering from a collection of uniform spheres of radius R can be described[23] by the form factor

$$f_s^2(QR) = \frac{9\pi}{2}\left(\frac{J_{3/2}(QR)}{(QR)^{3/2}}\right)^2 \quad (6)$$

The Bessel function $J_{3/2}(QR)$ is periodic, producing local maxima in $f_s^2(QR)$ at $QR = 5.765, 9.10, 12.33$, etc. In order to more fully describe the scattering behavior of our samples, we have adopted the methods developed by Hashimoto et al.[2] for including the effects of diffuse domain boundaries and a distribution in sphere sizes:

$$I_{obsd}(Q) = K(\rho_{bp} - \rho_{bm})^2 \times \left[\int_0^\infty P(R)R^6 f^2(Q,R)\,dR / \int_0^\infty P(R)\,dR\right] W(Q) \quad (7)$$

K is a constant that includes such factors as particle concentration and beam intensity, and $W(Q)$ is an interparticle interference function.[24] The effects of a diffuse domain boundary have been accounted for by modifying $f_s(QR)$

$$f(QR) = f_s(QR)\exp(-\sigma^2 Q^2/2) \quad (8)$$

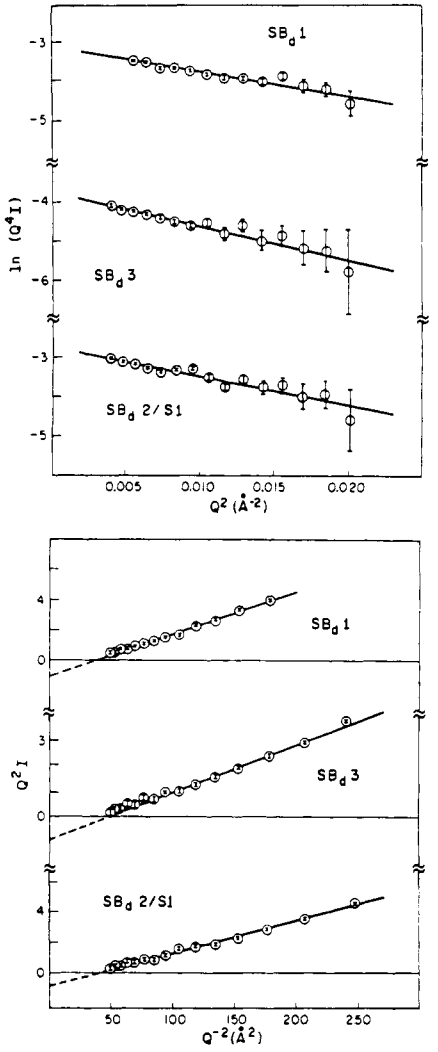

Figure 4. Porod plots[17] for the sigmoidal interfacial profile model (top) and the Helfand–Wasserman[7] profile model (bottom).

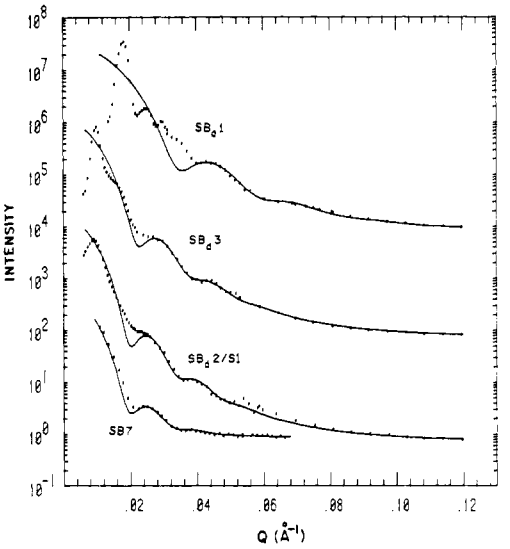

Figure 5. Radially averaged SANS intensities for four samples, together with scattering curves calculated assuming a collection of noninterfering spheres of mean radius $\bar{R}$ and a Gaussian distribution of sphere sizes characterized by σ_R, where $\bar{R}$ and σ_R were used as fitting parameters. Discrepancies at low Q are due to neglect of interparticle interference.

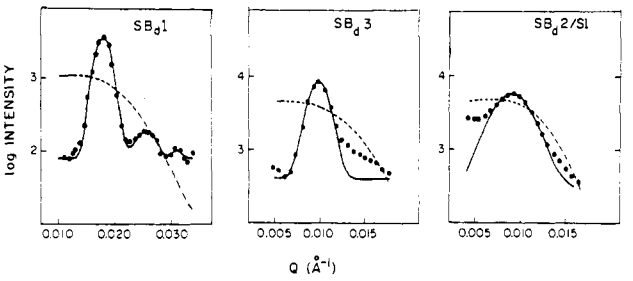

Figure 6. Low-Q SANS intensities compared with the interparticle interference (eq 10) from a randomly distributed ensemble of spheres (dashed line) and a set of Gaussian functions fit to the Bragg peaks (solid line).

where σ is taken from the Porod analysis. A Gaussian distribution in sphere sizes has also been assumed:

$$P(R) = (\text{constant}) \exp[-(R - \bar{R})^2/2\sigma_R^2] \quad (9)$$

Domain radii and size distributions have been determined by modeling SANS data with eq 7, using $\bar{R}$ and σ_R as fitting parameters and setting $W(Q)$ equal to unity.[2]

In all samples, good agreement was obtained between the model and data for $QR > 5$, as demonstrated in Figure 5. For some samples, particularly sample SB$_d$1, the model fails to describe the SANS features for $QR < 5$, a consequence of neglecting interparticle interference (see below). Domain dimensions determined by SANS are listed in Table IV. The slightly higher mean sphere-size distribution determined by SANS, $\langle\sigma_R/\bar{R}\rangle_{\text{SANS}} = 0.11$, vs. that from EM, $\langle\sigma_R/\bar{R}\rangle_{\text{EM}} = 0.08$ (Table II), can be attributed to neglecting instrument resolution effects in eq 7. Differences in $\bar{R}$ are discussed below.

Domain Packing. Interparticle interference from a randomly distributed ensemble of spherical particles can be described by[23]

$$W(Q) = \left(1 + \frac{V_0}{V_1} f_s(2QR)\right)^{-1} \quad (10)$$

where V_0/V_1 is the volume fraction of spheres. Therefore the simulations shown in Figure 5 have been modified by eq 10, and the low-Q results are plotted (dashed lines) with the SANS data in Figure 6. With the possible exception of sample SB$_d$2/S1, this modification fails to explain the interparticle scattering behavior of the samples. Thus a paracrystalline structure of the type described by Hosemann and Bagchi[24] is indicated

$$W(Q) = Z(Q)^*|S(Q)|^2 \quad (11)$$

where $Z(Q)$ represents the paracrystalline lattice factor, $S(Q)$ is the paracrystal shape amplitude, and the asterisk signifies a convolution product.

The local maxima in intensity apparent in sample SB$_d$1 (and to a lesser extent in SB$_d^3$ and SB$_d$2/S1) can be interpreted in terms of Bragg scattering from a mosaic of paracrystals; i.e., a Debye–Scherrer powder pattern is observed.[25] Each peak is associated with a paracrystalline planar spacing $\bar{D}$, as described by Bragg's law:

$$2\bar{D} \sin\theta = \lambda \quad (12)$$

Such planar spacings have been measured by fitting the resolvable peaks with Gaussian functions

$$I_{\text{Bragg}}(Q) = \sum c_i \exp\left[-\tfrac{1}{2}\left(\frac{Q - q_i}{\sigma_i}\right)^2\right] \quad (13)$$

added to an arbitrary background, as indicated by the solid curves in Figure 6. $\bar{D}$ spacings corresponding to the main Bragg peak in each sample are listed in Table IV. A discussion of the higher order reflections evident in sample SB$_d$1 has been presented elsewhere.[26]

The mean paracrystallite size in a given sample may be estimated from the Bragg peaks in a powder pattern by using a modified Scherrer formula. Assuming a spherical geometry, the paracrystallite radius is given by[27]

$$\bar{R}_{\text{crystal}} = 0.277\lambda/(B \cos \theta) \quad (14)$$

where B is the full width at half-maximum intensity (in radians) of the Bragg peak observed at a mean scattering angle of 2θ. Values for B ($=2.354\sigma$) have been obtained from the best fit of eq 13 to the first interference maximum (Figure 6). The number of domains per paracrystal can then be calculated from $\bar{R}_{\text{crystal}}$, $\bar{R}_{\text{sphere}}$, and the volume fraction of polybutadiene as determined by UV absorption. These values are also given in Table IV.

The influence of multiple-scattering effects on the Porod and domain size measurements in spherical domains has been shown[28] to be related to the total scattering probability.

$$\frac{s(0)}{k_0^2} = \frac{Dp(6\pi^2)R}{k_0^2}(\rho_{\text{bp}} - \rho_{\text{bm}})^2 \quad (15)$$

where p is the volume fraction of spheres, k_0 is the wavenumber, and D is the sample thickness. For the samples examined, $s(0)k_0^2 < 0.55$, which should result in less than a 2% error due to multiple scattering in the measurements.[28] In fact, no significant difference in interfacial thickness was found between the thick (0.2 cm) and thin (0.05 cm) specimen of sample SB_d1-M (Table IV). Also, $\sigma_R/\bar{R}$ for sample SB7 lies within the range of values determined for the deuterated samples having 27 times the total scattering probability. Therefore, multiple-scattering corrections to the SANS data were not considered necessary.

Discussion

Domain Boundary. Polymer–polymer interfaces have been a topic of intense theoretical discussion for more than a decade.[9,19,29-35] In particular, Helfand has published extensively on the subject with Tagami,[32,33] Sapse,[34] and Wasserman.[9,19] According to these authors, the density pattern of polymer B across a symmetric interface is given by

$$\rho_{\text{B}}(x) = \tfrac{1}{2}(1 - \tanh(2x/a_{\text{I}})) \quad (16)$$

Neglecting nonlocal interactions[34]

$$a_{\text{I}} = 2\left(\frac{\beta_{\text{A}}^2 + \beta_{\text{B}}^2}{2\alpha}\right)^{1/2} \quad (17)$$

$$\beta_{\text{K}}^2 = (1/6)\rho_{0\text{K}}b_{\text{K}}^2 \quad (18)$$

where $\rho_{0\text{K}}$ and b_{K} are the density and Kuhn statistical length, respectively, of segment K and α is the polymer–polymer interaction parameter. The modified version of Porod's law given by eq 3 was derived from the interfacial composition profile of eq 16.

The physical parameters $\rho_{0\text{K}}$ and b_{K} have been reported in the literature[19] for polystyrene and polybutadiene as follows:

$$\rho_{0\text{S}} = 10.1 \times 10^3 \text{ mol/m}^3 \qquad b_{\text{S}} = 6.8 \text{ Å}$$

$$\rho_{0\text{B}} = 16.5 \times 10^3 \text{ mol/m}^2 \qquad b_{\text{B}} = 6.3 \text{ Å}$$

Roe and Zin[35] have determined the pair interaction parameter Λ for polystyrene and 1,4-polybutadiene, which they found to be a weak function of temperature (°C) and composition, ϕ:

$$\Lambda_{\text{SB}} = \lambda_0 + \lambda_1\phi_1 + \lambda_T T \quad (\text{cal/cm}^3) \quad (19)$$

The constants appearing in eq 19 were averaged over all the reported values and with 95% confidence limits are given by $\lambda_0 = 0.996 \pm 0.174$, $\lambda_1 = 0.040 \pm 0.243$, and $\lambda_T = -0.00200 \pm 0.00116$. Therefore at 25 °C and $\phi = 0.5$

$$\alpha_{\text{SB}} = \Lambda_{\text{SB}}/RT = 1.63 \times 10^3 \ (\pm 22\%) \quad (\text{mol/m}^3) \quad (20)$$

This value is nearly identical with that calculated according to Rounds[37] ($\alpha = 1.62 \times 10^3$ mol/m^3 ± 72% at 25 °C), although Roe and Zin have provided a substantial improvement in precision.

The absence of nonlocal interaction terms in eq 17 is justified[34] since $\alpha/\rho_0 \ll 3$. Based on the above physical parameters, the interfacial thickness is calculated to be $a_{\text{I,predicted}} = 15 \pm 2$ Å, in excellent agreement with the experimentally determined values (Table IV). Also, since a_{I} is dominated by local interactions, it is not surprising to find that this parameter is insensitive to changes in the solvent-casting parameters.

Hashimoto et al.[1,2,4] have examined the domain boundary in a set of polystyrene–vinylpolyisoprene (SI) diblock copolymers and blends by SAXS. In agreement with the present study, they found that the interfacial thickness is essentially independent of molecular weight, homopolymer content, and casting solvent, although their value of $\Delta R \simeq 18$ Å is slightly smaller than that presently reported, $\Delta R \simeq 22$ Å. This variation can be explained in terms of the differences in physical parameters between the two systems. Parameters $\rho_{0\text{K}}$ and b_{K} have been measured[1] for vinylpolyisoprene but the interaction parameter for the polystyrene–vinylpolyisoprene pair has not been reported. According to eq 17, the differences in interfacial thickness can be accounted for if $\alpha_{\text{SI}} = 1.13\alpha_{\text{SB}}$, a difference qualitatively indicated in a recent publication by Cohen and Wilfong.[38]

Finally, as noted by Helfand and Wasserman,[19] the interfacial thickness obtained from a Gaussian smoothing function model, ΔR, cannot be directly compared with a_{I}, a point overlooked by Hashimoto et al.[1,2,4,6] Based on the results given in Table IV, these parameters are related by the proportionality constant

$$a_{\text{I}} \approx 0.68\Delta R \quad (21)$$

Domain Size. As reported elsewhere,[16] a discrepancy has been found between the measurement of polybutadiene sphere radius by electron microscopy and SANS. We believe that this is an artifact of microscopy, possibly related to staining, ultramicrotoming, or high-energy electron beam damage. Similar effects have recently been found in chlorosulfonic acid stained polypropylene.[39] Since the SANS experiment is carried out on an unperturbed sample of macroscopic dimensions and since sphere size determination is relatively direct and unambiguous, the SANS radii are accepted as correct and the EM radii have been corrected by a factor of 1.3 (see ref 16). Corrected EM radii (Table II) and SANS radii (Table IV) are plotted in Figure 7 as a function of rubber molecular weight.

Also plotted in Figure 7 (lower set of solid points) are the SANS results of Hashimoto et al.[2] obtained on a series of polystyrene–vinylpolyisoprene diblock copolymers (SI) containing spherical domains. The theoretical prediction[7] (Table II) for the domain radius of each sample examined in this study is also plotted in Figure 7 (upper set of solid points). For the case of blends containing homopolystyrene, the theoretical calculations were based on true polybutadiene weight fractions and molecular weights, with the assumption that the samples consisted of pure diblock copolymer. This was necessary because the theory[7] does

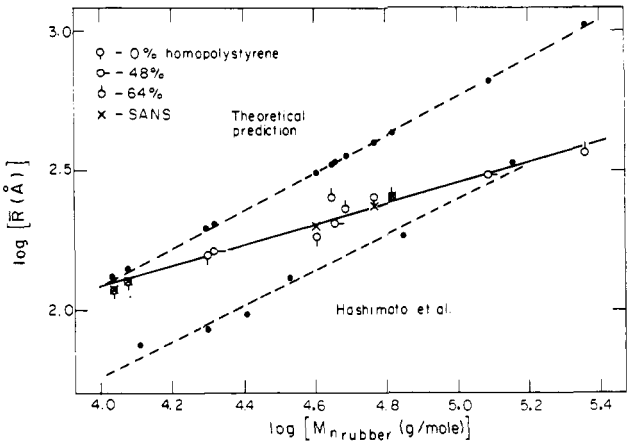

Figure 7. log–log plot of mean sphere size $\bar{R}$ vs. the molecular weight M_n of the rubber block for SB samples examined in the present study and SI diblocks studied by Hashimoto et al.[2] The upper dashed line has the 0.68 slope based on Helfand and Wasserman's results.[7] The solid line represents the best fit to values obtained in this study by electron microscopy[16] (open circles) and SANS (crosses) and has a slope of 0.37. The lower dashed line is fit to the results of Hashimoto et al.[2] and has a slope of 0.63.

not allow for the presence of homopolymer. Nevertheless, this assumption seems reasonable since the spherical domains consist entirely of block polybutadiene. Each of the three separate sets of points in Figure 7 can be well represented by

$$\bar{R} = (\text{constant}) M^{\beta}_{\text{rubber}} \tag{22}$$

where $\beta_B = 0.37$ (this work), $\beta_I = 0.63$ (Hashimoto's results[2]), and $\beta_H = 0.68$ (estimated from a linear-regression calculation based on Helfand and Wasserman's results[7]).

Solvent-cast block copolymers in the bulk state generally reflect a nonequilibrium morphology established in a solvated state. As pointed out by Hashimoto et al.,[2] in the case of spherical domains the bulk domain size reflects the number of chains per sphere, N, established at a particular solvent concentration, ϕ. Variations in N with further reduction in solvent content require the transport of SB (or SI) chains in a two-phase system; this is prevented by an energy barrier which cannot be overcome once phase separation has occurred. Using such arguments, Hashimoto et al. qualitatively explained the form of their data shown in Figure 7; their SI diblocks and their casting procedures led to formation of spherical domains that were smaller than expected by a constant factor over the entire range of molecular weight studied. Our results on SB diblocks shown in Figure 7 also deviate from prediction in the expected direction; the polybutadiene domains are always smaller than predicted. However, the departure from theoretical prediction is exceedingly small at low molecular weights but it increases at higher molecular weights. This result is intuitively satisfying since it is more likely that equilibrium structures will be formed at the lower end of the molecular weight scale. Furthermore the higher casting temperature used in the present study (80 °C vs. 30 °C in the work of Hashimoto et al.[2]) and the lower rubber content (12% vs. 17%) of our block copolymers both tend to favor the production of bulk equilibrium structures from solvent casting. Semiquantitative support for these arguments has been presented elsewhere[9] using the concept of a block copolymer–solvent phase separation temperature T (and its dependence on copolymer composition and molecular weight) which was originally developed by Pico and Williams.[40]

The fact that samples SB_d1 and SB_d3 exhibit little or no change in sphere size as casting solvent is varied (Table IV) is consistent with the findings of Hashimoto et al.[4] According to Pico and Williams,[40] ϕ_S is relatively insensitive to solvent type as long as the solubility parameter of the solvent is close to the range of the two blocks. Such is the case for the solvents and casting temperatures employed here.

Domain Packing. In a previous paper[26] we have shown that the three Bragg peaks associated with sample SB_d1 (Figure 6) are reflections from the (110), (200), and (211) planes of a set of body-centered-cubic (bcc) paracrystals, in accordance with the equilibrium prediction of Leibler.[41] Increasing block molecular weight (sample SB_d3) reduces this to one resolvable interference maximum, to which we can ascribe no specific packing mode. Correspondingly, the number of domains per paracrystal has dropped from over 100 for SB_d1 to about 40 for SB_d3. While it is tempting to also attribute these results to the departure of domain size in SB_d3 from equilibrium (Figure 2), there is no clear reason why decreasing N should also affect the packing order. On the other hand, the increase in solution viscosity associated with raising the molecular weight can perhaps account for the observed behavior.

Nearly complete loss of order is displayed by sample $SB_d2/S1$ and accordingly, the SANS results are nearly predicted by the interparticle interference function given by eq 10. In this case, neither the value of N nor solution viscosity can be responsible, since $SB_d2/S1$ and SB_d3 exhibit similar bulk sphere radii. Thus the nearly complete absence of paracrystallinity in sample $SB_d2/S1$ is due to the presence of homopolystyrene.[3]

Conclusions

The bulk equilibrium structural characteristics of diblock copolymers of the type discussed in this work (spherical microstructure) can be accurately predicted from theory. This has been demonstrated for two of the samples studied, SB_d1 and SB1, where Leibler[41] correctly predicts a bcc macrolattice, Helfand and Wasserman[7] specify the sphere radius to within 10%, and Helfand et al.[32-34] exactly predict the domain boundary thickness. Variations in block polymer molecular weight, blending with matrix homopolymer, and sample preparation by solvent casting influence each of these structural features in a different way. The domain boundary thickness is dictated entirely by local interactions and accordingly is not affected by any of these factors. Blending with matrix homopolymer has no influence on domain size but leads to nearly complete loss of paracrystallinity. Solvent casting can dramatically affect bulk domain dimensions, as demonstrated by the 0.37 power dependence of sphere radius on block molecular weight, in sharp contrast to the expected equilibrium value of 0.68. Understanding these processes permits us to critically determine the validity and range of applicability of bulk equilibrium theories as stated above and provides an added dimension of control over the structural features attainable with these materials.

Acknowledgment. We are very grateful to Chris Schwier for his invaluable assistance in polymer synthesis and many helpful discussions and to Dr. George Wignall of NCSASR for his help. This research has been supported by the National Science Foundation, Division of Materials Research, Polymers Program, under Grant DMR-8001674. SANS experiments were performed at the National Center for Small-Angle Scattering Research, which is funded by NSF Grant DMR-7724458 through interagency agreement 406377-77 with DOE.

Registry No. Homopolystyrene, 9003-53-6; butadiene–styrene copolymer, 9003-55-8.

References and Notes

(1) Hashimoto, T.; Shibayama, M.; Kawai, H. *Macromolecules* **1980**, *13*, 1237.
(2) Hashimoto, T.; Fujimura, M.; Kawai, H. *Macromolecules* **1980**, *13*, 1660.
(3) Fujimura, M.; Hashimoto, H.; Kurashashi, K.; Hashimoto, T.; Kawai, H. *Macromolecules* **1981**, *14*, 1196.
(4) Hashimoto, H.; Fujimura, M.; Hashimoto, T.; Kawai, H. *Macromolecules* **1981**, *15*, 844.
(5) Hashimoto, T.; Shibayama, M.; Kawai, H. *Polym. Prepr., Am. Chem. Soc., Div. Polym. Chem.* **1982**, *23* (1), 21.
(6) Hashimoto, T.; Todo, A.; Itoi, H.; Kawai, H. *Macromolecules* **1977**, *10* (2), 377.
(7) Helfand, E.; Wasserman, Z. *Macromolecules* **1978**, *11*, 960.
(8) Bates, F. S.; Berney, C. V.; Cohen, R. E.; Wignall, G. D. *Polymer* **1983**, *24*, 519.
(9) Bates, F. S. Sc.D. Thesis, Massachusetts Institute of Technology, 1982.
(10) Eppley, R. L.; Dixon, J. A. *J. Organomet. Chem.* **1967**, *8*, 176.
(11) Geerts, J.; Van Beylen, M.; Smets, G. *J. Polym. Sci., Part A-1* **1969**, *7*, 2805.
(12) Bates, F. S.; Cohen, R. E. *Macromolecules* **1981**, *14*, 881.
(13) Ramos, A. R.; Cohen, R. E. *Polym. Eng. Sci.* **1977**, *17*, 639.
(14) Kato, K. *Polym. Lett.* **1966**, *4*, 35.
(15) Koehler, W. C.; Hendricks, R. W.; Childs, H. R.; King, S. P.; Lin, S. S.; Wignal, G. D. "Scattering Techniques Applied to Supramolecular Systems"; Chen, S., Chu, B., Nossal, R., Eds.; Plenum Press: New York, 1981.
(16) Berney, C. V.; Bates, F. S.; Cohen, R. E. *Polymer* **1982**, *23*, 1222.
(17) Koberstein, J. T.; Morra, B.; Stein, R. S. *J. Appl. Crystallogr.* **1980**, *13*, 34.
(18) Ruland, W. *J. Appl. Crystallogr.* **1971**, *4*, 70.
(19) Helfand, E.; Wasserman, Z. R. "Developments in Block Copolymers"; Goodman, I., Ed.; Applied Science Publishers, Ltd., London, 1982; Chapter 4.
(20) Vonk, E. G. *J. Appl. Cryst.* **1973**, *6*, 81.
(21) Ruland, W. *Colloid Polym. Sci.* **1977**, *255* (5), 417.
(22) Wignall, G. D., personal communication.
(23) Guinier, A.; Fournet, G. "Small-Angle Scattering of X-Rays"; Wiley: New York, 1955.
(24) Hosemann, R.; Bagchi, S. N. "Direct Analysis of Diffraction by Matter"; North Holland Publishing Co.: Amsterdam, 1962.
(25) Cohen, J. B. "Diffraction Methods in Material Science"; Macmillan: New York, 1966.
(26) Bates, F. S.; Cohen, R. E.; Berney, C. V. *Macromolecules* **1982**, *15*, 589.
(27) Warren, B. E. *J. Appl. Crystallogr.* **1978**, *11*, 695.
(28) Schelten, J.; Schmatz, W. *J. Appl. Crystallogr.* **1980**, *13*, 385.
(29) Leary, D. F.; Williams, M. C. *Polym. Lett.* **1970**, *8*, 335.
(30) Leary, D. F.; Williams, M. C. *J. Polym. Sci., Polym. Phys. Ed.* **1973**, *11*, 345.
(31) Leary, D. F.; Williams, M. C. *J. Polym. Sci., Polym. Phys. Ed.* **1974**, *12*, 265.
(32) Helfand, E.; Tagami, Y. *Polym. Lett.* **1971**, *9*, 741.
(33) Helfand, E.; Tagami, Y. *J. Chem. Phys.* **1971**, *56*, 3592.
(34) Helfand, E.; Sapse, A. M. *J. Chem. Phys.* **1975**, *62*, 1327.
(35) Roe, R.-J.; Zin, W.-C. *Macromolecules* **1980**, *13*, 1221.
(36) Meier, D. J. *Polym. Prepn., Am. Chem. Soc., Div. Polym. Chem.* **1974**, *15*, 171.
(37) Rounds, N. A. Doctoral Dissertation, University of Akron, 1971.
(38) Cohen, R. E.; Wilfong, D. E., *Macromolecules* **1982**, *15*, 370.
(39) Stribeck, N. Ph.D. Dissertation, Phillips-Universität, Marburg/Lahn, 1980.
(40) Pico, E. R.; Williams, M. C. *J. Polym. Sci., Polym. Phys. Ed.* **1977**, *15*, 1585.
(41) Leibler, L. *Macromolecules* **1980**, *13*, 1602.

Dynamic Mechanical Properties of Polystyrene Containing Microspherical Inclusions of Polybutadiene: Influence of Domain Boundaries and Rubber Molecular Weight

Frank S. Bates,† R. E. Cohen,* and A. S. Argon

Department of Chemical Engineering and Department of Mechanical Engineering, Massachusetts Institute of Technology, Cambridge, Massachusetts 02139.
Received October 27, 1982

ABSTRACT: A model set of well-characterized anionically polymerized diblock copolymer–homopolymer blends was prepared from styrene and butadiene. These materials contain microspherical polybutadiene domains whose phase boundary thickness, size, size distribution, and spatial packing are all known from previous electron microscopy and small-angle neutron scattering studies of the same set of samples. Dynamic mechanical properties were determined in a tensile mode at 3.5 Hz between −140 and +110 °C. Increasing the volume fraction of interfacial material in these composites produces no change in the storage modulus and a small increase in the level of viscoelastic loss in the region between the pure-component glass transition temperatures. Inclusion of polybutadiene in a glassy polystyrene matrix results in a significant lowering of the rubber glass transition temperature, T_g^B, which can be explained on the basis of negative pressure resulting from differential contraction. Composites containing lower molecular weight polybutadienes exhibit smaller T_g^B depressions, suggesting the possibility of cavitation in the rubber in these materials.

Introduction

Although the dynamic mechanical behavior of block copolymers and polymer blends comprised of polystyrene and polybutadiene has been widely investigated, clear interpretation of the mechanical results has often been impossible owing to the lack of extensive molecular, interfacial, and morphological characterization data on the full set of samples under investigation. Conflicting conclusions have been reported on the influence of various structural features of these materials on the dynamic mechanical behavior. This is particular true for the role of the interfacial zone, the structural feature that is most difficult to quantify and therefore most open to speculation in terms of its effect on mechanical properties.

A series of microheterogenous composites based on block copolymers and homopolymers of polystyrene and polybutadiene has been under investigation in our laboratories. Primary focus has been on structural characterization via neutron scattering and electron microscopy (see paper

†Present address: Bell Laboratories, Murray Hill, NJ 07974.

0024-9297/83/2216-1108$01.50/0